Research Article

Journal of PeptideScience

Received: 20 April 2010 Revised: 25 May 2010 Accepted: 2 June 2010 Published online in Wiley Online Library: 20 July 2010

(wileyonlinelibrary.com) DOI 10.1002/psc.1268

Candidacidal mechanism of a Leu/Lys-rich α-helical amphipathic model antimicrobial peptide and its diastereomer composed of D,L-amino acids

Peng Wang,[a] Yong Hai Nan[a] and Song Yub Shin[a,b]*

We investigated the mechanism of candidacidal action of a Lys/Leu-rich α-helical model antimicrobial peptide (K_9L_8W) and its diastereomeric peptide (D_9-K_9L_8W) composed of D,L-amino acids. K_9L_8W killed completely *Candida albicans* within 30 min, but D_9-K_9L_8W killed only 72% of *C. albicans* even after 100 min. Tryptophan fluorescence spectroscopy indicated that the fungal cell selectivity of D_9-K_9L_8W is closely correlated with a selective interaction with the negatively charged PC/PE/PI/ergosterol (5 : 2.5 : 2.5 : 1, w/w/w/w) phospholipids, which mimic the outer leaflet of the plasma membrane of *C. albicans*. K_9L_8W was able to induce almost 100% calcein leakage from PC/PE/PI/ergosterol (5 : 2.5 : 2.5 : 1, w/w/w/w) liposomes at a peptide : lipid molar ratio of 1 : 16, whereas D_9-K_9L_8W caused only 25% dye leakage even at a peptide : lipid molar ratio of 1 : 2. Confocal laser-scanning microscopy revealed that FITC-labeled D_9-K_9L_8W penetrated the cell wall and cell membrane and accumulated inside the cells, whereas FITC-labeled K_9L_8W did not penetrate but associated with the membranes. Collectively, our results demonstrated that the candidacidal activity of K_9L_8 W and D_9-K_9L_8W may be due to the transmembrane pore/channel formation or perturbation of the fungal cytoplasmic membranes and the inhibition of intracellular functions, respectively. Finally, D_9-K_9L_8W with potent anti-*Candida* activity but no hemolytic activity may be potentially a useful lead compound for the development of novel antifungal agents. Copyright © 2010 European Peptide Society and John Wiley & Sons, Ltd.

Keywords: Leu/Lys-rich α-helical model antimicrobial peptide; diastereomeric peptide; candidacidal activity; candidacidal mechanism

Introduction

Antimicrobial peptides (AMPs) are widely distributed throughout the animal and plant kingdoms [1]. They are recognized as an important component of the innate immunity and host defense against microbial infections [2,3]. Majority of AMPs have been categorized into four distinct structural classes: α-helices, β-sheets, extended helices and loops [4]. The most abundant structural class in naturally occurring AMPs is an amphipathic α-helix [5]. Most of the AMPs kill bacteria by permeabilizing the target cell membrane. Their net positive charge presumably facilitates interactions with negatively charged moieties present in membranes and/or bacterial cell walls, whereas their amphipathic character enables membrane penetration and permeabilization [6].

On the basis of their cell selectivity, α-helical AMPs can be distinguished into two classes: cell-selective α-helical AMPs (e.g. magainins and cecropins), which have lytic activity against bacterial cells only, and non-cell-selective α-helical AMPs (e.g. melittin and pardaxin), which have lytic activity against both bacterial and mammalian cells (e.g. human red blood cells) [5,7–11]. Several studies demonstrated that the introduction of D-amino acids in non-cell-selective α-helical natural or designed AMPs causes a loss of their hemolytic activity but retains their antimicrobial activity [7,9,12–19].

Recently, we designed and synthesized an amphipathic α-helical model non-cell-selective AMP (K_9L_8W) composed of nine lysines, eight leucines and one tryptophan and its diastereomeric peptide (D_9-K_9L_8W) composed of D,L -amino acids [20]. D_9-K_9L_8W showed much higher cell selectivity compared with K_9L_8W. D_9-K_9L_8W (MIC: 2–4 μM) displayed two- to fourfold higher antimicrobial activity against Gram-positive and Gram-negative bacteria as compared with K_9L_8W (MIC: 4–8 μM). K_9L_8W displayed relatively high hemolytic activity inducing 50% hemolysis at 14 μM, whereas D_9-K_9L_8W did not induce any hemolysis even up to 800 μM.

Candida albicans is an opportunistic fungal pathogen that is a leading cause for mucosal and systemic candidiasis in people [21,22]. The cytotoxicity of antifungal agents and the emergence of strains resistant to currently used antifungal drugs, such as fluconazole and amphotericin B [23], have renewed interest in the development of novel approaches to the design of peptide-based antifungal agents that are less harmful for host cells and that possess a low tendency to induce resistance. A number of antimicrobial peptides, including histatin 5, lactoferrin-derived peptides and cathelicidin peptides, have shown potent fungicidal activities against *C. albicans* [24–26].

In this study, we found that K_9L_8W and D_9-K_9L_8W have a potent antifungal activity against *C. albicans* with MIC ranging between

* *Correspondence to: Song Yub Shin, Department of Cellular & Molecular Medicine, School of Medicine, Chosun University, Gwangju 501-759, Repulic of Korea. E-mail: syshin@chosun.ac.kr*

a *Department of Bio-Materials, Graduate School, Chosun University, Gwangju 501-759, Republic of Korea*

b *Department of Cellular & Molecular Medicine, School of Medicine, Chosun University, Gwangju 501-759, Republic of Korea*

Table 1. Amino acid sequences, calculated and observed molecular masses, anti-*Candida* activity and hemolytic activity of the peptides

Peptides	Amino acid sequences	Molecular MS		*Candida albicans* MIC (μM)	Human red blood cells HC_{50} (μM)[b]
		Calculated	Measured[a]		
K_9L_8W	**KLKKLLKKWLKLLKKLLK-NH_2**	2262.1	2261.9	8–16	14[c]
D_9-K_9L_8W	**KlKkLlKkWlKlLkKlLk-NH_2**	2262.1	2261.7	8–16	<800[c]

Small and underlined letters represent D-amino acids.
[a] Molecular masses were determined by MALDI-TOF-MS.
[b] HC_{50} displays the peptide concentration that causes 50% hemolysis.
[c] These values are taken from our previous study [20].

8 and 16 μM. To investigate the molecular basis for the selectivity of the peptides between the fungal and mammalian cells, we examined the interaction of the peptides with model liposome systems mimicking the fungal and mammalian cytoplasmic membranes. Furthermore, in order to elucidate the mechanism of candidacidal action of K_9L_8W and D_9-K_9L_8W, we examined the leakage of calcein from PC/PE/PI/ergosterol (5 : 2.5 : 2.5 : 1, w/w/w/w) liposomes, which mimic the outer leaflet of the plasma membrane of *C. albicans* and visualized the association of the peptides with *C. albicans* by confocal laser-scanning microscopy.

Materials and Methods

Materials

Rink amide 4-methylbenzhydrylamine (MBHA) resin, Fmoc-amino acids and other reagents for the peptide synthesis were purchased from Calbiochem-Novabiochem (La Jolla, CA). Posphatidylcholine (PC, from egg yolk), phosphatidylglycerol (from egg yolk), phosphatidylethanolamine (PE, from egg yolk), phosphatidylinositol (PI, from soybean), cholesterol, ergosterol, acrylamide and calcein were supplied from Sigma Chemical Co (St. Louis, MO). All other reagents were of analytical grade. The buffers were prepared in double-glass distilled water.

Peptide Synthesis

The peptides and FITC-labeled peptides were prepared by the standard Fmoc-based solid-phase synthesis technique on a solid support of Rink amide MBHA resin. DCC and HOBt were used as coupling reagent, and tenfold excess Fmoc-amino acids were added during every coupling cycle. After cleavage and deprotection with a mixture of trifluoroacetic acid/water/thioanisole/phenol/ethanedithiol/triisopropylsilane (81.5 : 5 : 5 : 5 : 2.5 : 1, v/v/v/v/v/v) for 2 h at room temperature, the crude peptides were repeatedly extracted with diethyl ether and purified by reverse-phase HPLC on a preparative Vydac C_{18} column (15 μm, 20 × 250 mm) using an appropriate 0–90% water/acetonitrile gradient in the presence of 0.05% trifluoroacetic acid. The final purity of the peptides (>98%) was assessed by reverse-phase HPLC on an analytical Vydac C_{18} column (4.6 × 250 mm, 300 Å, 5-μm particle size). The molecular mass of the purified peptides was determined by MALDI-TOF-MS (Shimadzu, Japan) (Table 1).

Anti-*Candida* Activity and Kinetics

Anti-fungal activity of the peptides against *C. albicans* (KCTC 7965) was determined by the broth microdilution susceptibility assay. Briefly, single colonies of *C. albicans* were inoculated into the culture media (YPD broth) (2% dextrose, 1% peptone and 0.5% yeast extract) and cultured overnight at 28 °C. An aliquot of these cultures were transferred to 10-ml fresh culture medium and incubated for an additional 3–5 h at 28 °C to obtain mid-logarithmic phase organisms. A twofold dilution series of peptides in phosphate-buffered saline (PBS) was prepared. A set of serial dilutions (100 μl) were added to 100 μl of 1×10^5 CFU/ml in 96-well microtiter plates (Falcon) and then incubated at 28 °C for 16 h. The lowest concentration of peptide that completely inhibited growth of the organisms was defined as the MIC. The MICs were the average of triplicate measurements in three independent assays. *Candida albicans* (KCTC 7965) was procured from the Korean Collection for Type Cultures (KCTC) at the Korea Research Institute of Bioscience and Biotechnology.

The kinetics of anti-*Candida* activity of the peptides was assessed at a peptide concentration of 16 μM. The initial density of *C. albicans* was approximately 1×10^5 CFU/ml. After 0, 10, 30, 60 or 100 min of exposure to the peptides at 28 °C, 50 μl aliquots of the serial tenfold dilutions (up to 10^{-3}) of the cultures were plated into YPD agar plates to assess their viability. Colonies were counted after incubation for 24 h at 28 °C.

Preparation of Small Unilamellar Vesicles

Small unilamellar vesicles (SUVs) were prepared by sonication as described earlier [27]. Briefly, dry lipids were dissolved in chloroform in a small glass vessel. Solvents were removed by rotary evaporation to form a thin film on the wall of a glass vessel and lyophilized overnight. Dried thin films were resuspended in Tris–HCl buffer by vortex mixing. Lipid dispersions were sonicated on ice water for 10–20 min with a titanium-tip ultrasonicator until the solution became transparent. Two different compositions of lipid films were prepared: PC/PE/PI/ergosterol (5 : 2.5 : 2.5 : 1, w/w/w/w) and PC/cholesterol (10 : 1, w/w), which mimic the outer leaflet of the plasma membrane of *C. albicans* [28,29] and human red blood cells [30], respectively.

Tryptophan Fluorescence Blue Shift

The fluorescence emission spectrum of tryptophan of the peptides was monitored in aqueous Tris–HCl buffer and in the presence of vesicles composed of either PC/PE/PI/ergosterol (5 : 2.5 : 2.5 : 1, w/w/w/w) SUVs or PC/cholesterol (10 : 1, w/w) SUVs. In these fluorometric studies, SUVs were used to minimize differential light scattering effects [27,31]. Tryptophan fluorescence measurements were obtained using a model RF-5301PC spectrophotometer (Shimadzu). Each peptide was added to 3 ml of Tris–HCl buffer (10 mM Tris, 0.1 mM EDTA, 150 mM NaCl, pH 7.4) containing 0.6 mM

Journal of PeptideScience

liposomes (pH 7.4), and the peptide/liposome mixture (molar ratio of 1 : 200) allowed to interact at 20 °C for 10 min. The fluorescence was excited at 280 nm, and emission scanned from 300 to 400 nm.

Quenching of Trp Emission by Acrylamide

For fluorescence quenching experiment, acrylamide was used as the quencher and the fluorescence measurements were taken with a model RF-5301PC spectrophotometer (Shimadzu). To reduce absorbance by acrylamide, excitation of Trp at 295 nm instead of 280 nm was used [32,33]. Aliquots of the 3.0 M solution of this water-soluble quencher were added to the peptide in presence of 0.6 mM PC/PE/PI/ergosterol (5 : 2.5 : 2.5 : 1, w/w/w/w) SUVs at a peptide/lipid molar ratio of 1 : 200. The effect of acrylamide on the fluorescence of each peptide was analyzed by the Stern–Volmer equation: $F_0/F = 1 + K_{sv}$ [Q], where F_0 and F represent the fluorescence intensities in the absence and presence of acrylamide, respectively, and K_{sv} is the Stern–Volmer quenching constant and [Q] is the concentration of acrylamide.

Dye Leakage

Calcein-entrapped large unilamellar vesicles (LUVs) composed of PC/PE/PI/ergosterol (5 : 2.5 : 2.5 : 1, w/w/w/w) were prepared by vortexing the dried lipid in dye buffer solution (70 mM calcein, 10 mM Tris, 150 mM NaCl, 0.1 mM EDTA, pH 7.4). The suspension was subjected to ten freeze–thaw cycles in liquid nitrogen and extruded 21 times through polycarbonate filters (two stacked 100-nm pore size filters) with a LiposoFast extruder (Avestin, Inc., Canada). Untrapped calcein was removed by gel filtration on a Sephadex G-50 column. The concentration of calcein-entrapped LUVs was determined in triplicate by phosphorus analysis [34]. Calcein leakage from LUVs was monitored by measuring fluorescence intensity at an excitation wavelength of 490 nm and an emission wavelength of 520 nm on a model RF-5301PC spectrophotometer. The maximum fluorescence intensity corresponding to 100% leakage was determined by addition of 10% (w/v) Triton X-100 (20 µl) to 2 ml of the sample. The percentage of dye leakage caused by the peptides was calculated as follows:

$$\%\ \text{Dye leakage} = 100 \times \left[\frac{(F - F_0)}{(F_t - F_0)}\right] \quad (1)$$

where F is the fluorescence intensity achieved at 3 min after peptide addition, and F_0 and F_t represent fluorescence intensities without the peptides and with Triton X-100, respectively.

Confocal Laser-Scanning Microscopy

Candida albicans cells were grown to the mid-logarithmic phase. The cells (1×10^6 CFU/ml) in 10 mM PBS, pH 7.4, were incubated with FITC-labeled peptides (10 µg/ml) at 28 °C for 30 min. Next, the cells were washed with PBS and immobilized on a glass slide. FITC-labeled peptides were observed with an Olympus IX 70 confocal laser-scanning microscope (Japan). Fluorescent images were obtained with a 488-nm band-pass filter for FITC excitation.

Results and Discussion

The α-helical model non-cell-selective antimicrobial peptide (K_9L_8W) and its diastereomeric peptide (D_9-K_9L_8W) showed the same MIC value ranging between 8 and 16 µM against *C. albicans*

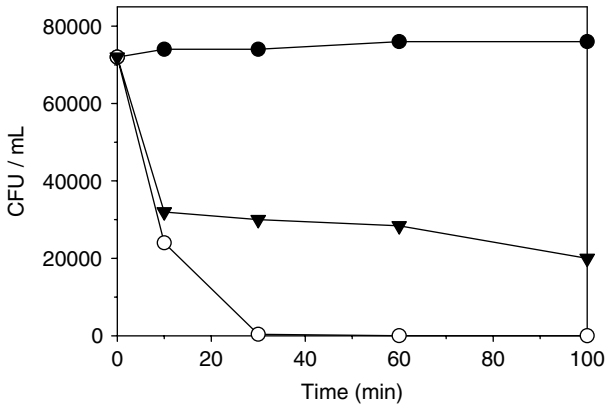

Figure 1. Kinetics of killing of the peptides against *Candida albicans*. *C. albicans* was incubated in the absence (●) and in the presence of K_9L_8W (○) or D_9-K_9L_8W (▼) in agar broth. The concentration of each peptide used was 16 µM.

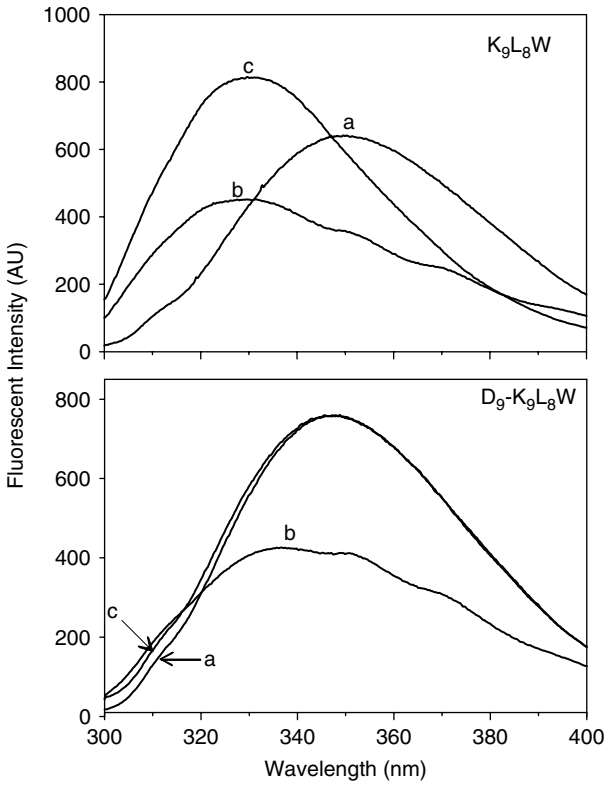

Figure 2. Fluorescence spectra of 3 µM peptides in Tris–HCl buffer (pH 7.2) (a) in the presence of PC/PE/PI/ergosterol (5 : 2.5 : 2.5 : 1, w/w/w/w) SUVs (b) and PC/cholesterol (10 : 1, w/w) SUVs (c).

(Table 1). Next, we investigated the kinetics of candidacidal activity to compare the rate at which these two peptides kill *C. albicans*. We compared the killing kinetics of K_9L_8W and D_9-K_9L_8W against *C. albicans* at intervals of 0, 10, 30, 60 and 100 min at 16 µM. As shown in Figure 1, K_9L_8W killed completely *C. albicans* within 30 min, but D_9-K_9L_8W killed 72.2% of *C. albicans* even after 100 min.

When excited at 280 nm in an aqueous buffer, Trp residues in the peptides gave rise to an emission peak centered at 350 nm. When the peptides were bound to phospholipids, the hydrophobic

Table 2. Tryptophan emission maxima and K_{sv} in Tris–HCl buffer or in the presence of liposomes of the peptides

Peptides	Tris–HCl buffer (pH 7.2) (nm)	PC/PE/PI/ergosterol (5 : 2.5 : 2.5 : 1, w/w/w/w) (nm)	PC/cholesterol (10 : 1, w/w) (nm)	K_{sv} (M^{-1})[b] Tris–HCl buffer (pH 7.2)	PC/PE/PI/ergosterol (5 : 2.5 : 2.5 : 1, w/w/w/w)	PC/cholesterol (10 : 1, w/w)
K_9L_8W	349.4	329.6 (19.8)	328.4 (21.0)[a]	7.75	1.29	2.03
D_9-K_9L_8W	348.8	336.6 (12.2)	347.2 (1.6)	9.69	1.53	4.27

Assays were carried out in Tris–HCl buffer or in the presence of PC/PE/PI/ergosterol (5/2.5/2.5/1, w/w/w/w) or PC/cholesterol (10 : 1, w/w) liposomes at a lipid/peptide molar ratio of 100 : 1.
[a] Blue shift in emission maximum in parentheses.
[b] K_{sv} is the Stern–Volmer quenching constant.

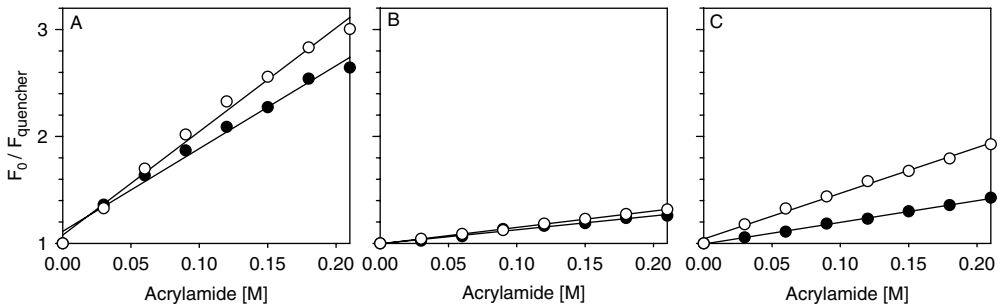

Figure 3. Stern–Volmer plots for the quenching of Trp fluorescence of the peptides by an aqueous quencher, acrylamide, in Tris–HCl buffer (pH 7.2) (A) in the presence of PC/PE/PI/ergosterol (5 : 2.5 : 2.5 : 1, w/w/w/w) SUVs (B) and PC/cholesterol (10 : 1, w/w) SUVs (C). Peptides are indicated as follows: K_9L_8W (●) and D_9-K_9L_8W (○).

environment and the decreased flexibility of the Trp residues caused a shift in this emission to lower wavelengths (blue shift). In negative charged PC/PE/PI/ergosterol (5 : 2.5 : 2.5 : 1, w/w/w/w) SUVs, the fluorescence emission maxima of K_9L_8W and D_9-K_9L_8W exhibited a large blue shift of 19.8 and 12.2, respectively, indicating that these two peptides penetrated into the hydrocarbon region of the bilayer of *C. albicans* (Figure 2 and Table 2). These results reflected potent anti-*Candida* activity of these two peptides. In zwitterionic PC/cholesterol (10 : 1, w/w) SUVs, D_9-K_9L_8W induced no blue shift in fluorescence emission maxima, whereas K_9L_8W produced a large blue shift of 21.0 (Figure 2 and Table 2). These data reflected high hemolytic activity of K_9L_8W.

To further investigate the relative extent of peptide penetration in liposomes and the lipid specificity of the peptide–liposome interaction, we examined the effect of acrylamide, a water-soluble neutral quencher of tryptophan fluorescence. Acrylamide is useful as a quenching agent because it does not interact with the head group of negatively charged phospholipids. The Stern–Volmer plots for the quenching of tryptophan by acrylamide in Tris–HCl buffer or in the presence of PC/PE/PI/ergosterol (5 : 2.5 : 2.5 : 1, w/w/w/w) SUVs or PC/cholesterol (10 : 1, w/w) SUVs are depicted in Figure 3. The tryptophan fluorescence for K_9L_8W and D_9-K_9L_8W was decreased in a concentration-dependent manner by the addition of acrylamide. In negatively charged PC/PE/PI/ergosterol (5 : 2.5 : 2.5 : 1, w/w/w/w) liposomes, both K_9L_8W and D_9-K_9L_8W showed similar slopes and K_{sv}. In contrast, in zwitterionic PC/cholesterol (10 : 1, w/w) liposomes, D_9-K_9L_8W exhibited a higher slope and larger K_{sv} than K_9L_8W, suggesting that the Trp residue of D_9-K_9L_8W is less anchored within the hydrophobic core of the zwitterionic phospholipids compared with K_9L_8W. Therefore, tryptophan fluorescence blue shift and quenching studies indicated that the fungal cell selectivity of D_9-K_9L_8W is closely correlated with a selective interaction with

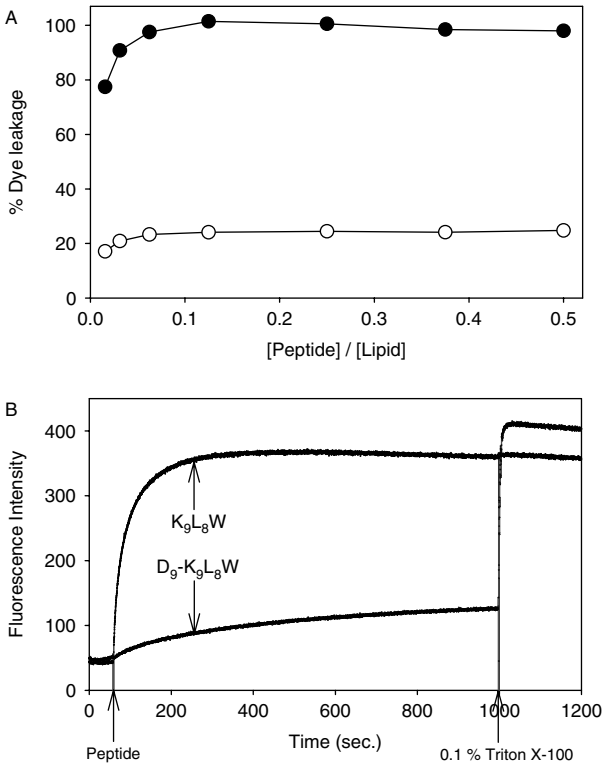

Figure 4. (A) Concentration-dependent leakage of calcein from PC/PE/PI/ergosterol (5 : 2.5 : 2.5 : 1, w/w/w/w) LUVs. Peptides are indicated as follows: K_9L_8W (●) and D_9-K_9L_8W (○). (B) Time-dependent leakage of calcein from PC/PE/PI/ergosterol (5 : 2.5 : 2.5 : 1, w/w/w/w) LUVs. The concentration of the peptides was 8 μM. The concentration of the liposome was 64 μM.

Journal of PeptideScience

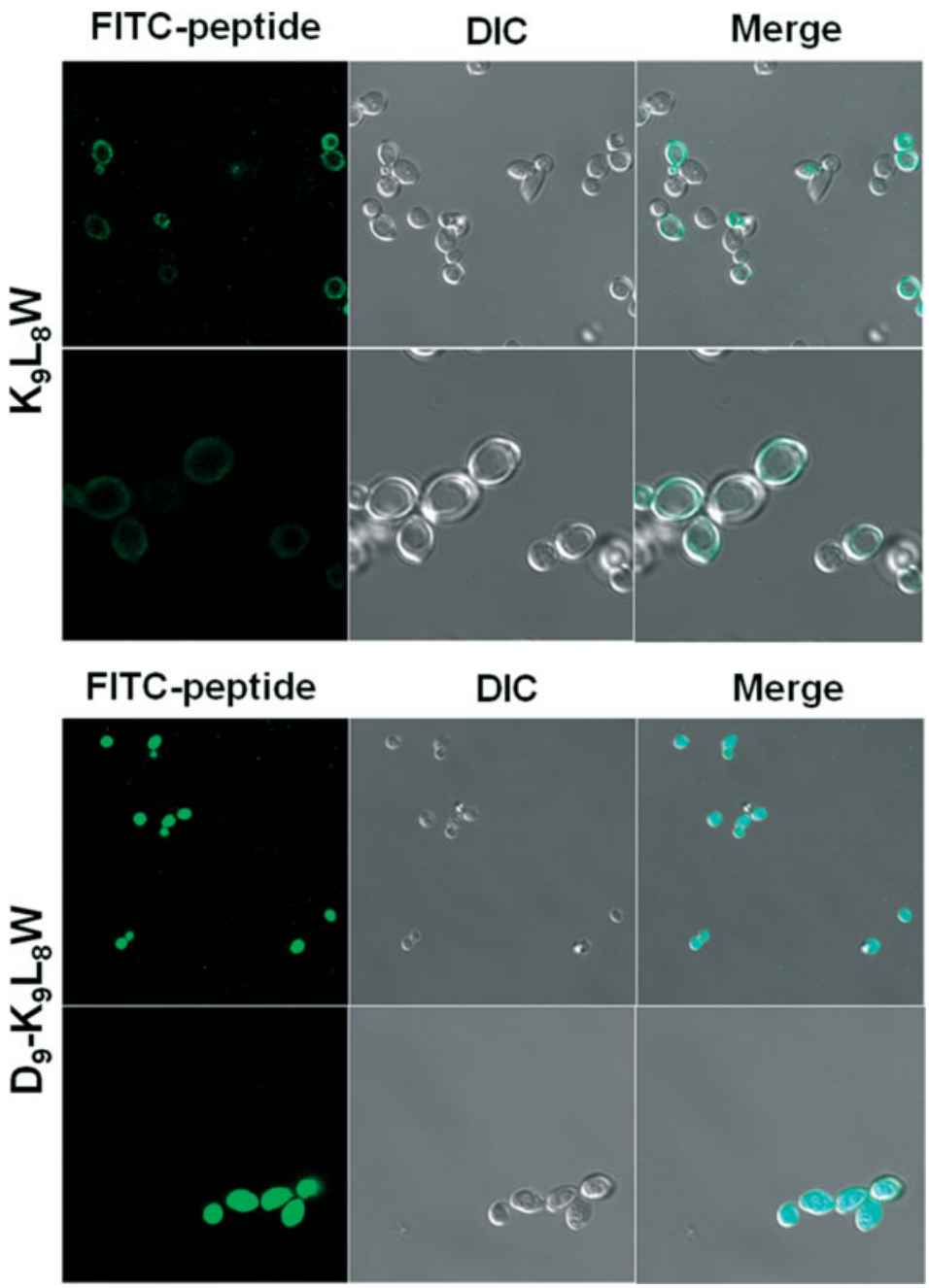

Figure 5. Detection of localization of the FITC-labeled K_9L_8W and FITC-labeled D_9-K_9L_8W onto *Candida albicans* by confocal laser-scanning microscopy. *C. albicans* cells were incubated with 10 μg/ml FITC-labeled peptides at 28 °C for 30 min. For each peptide treatment, fluorescence, DIC and merge images are shown.

negatively charged PC/PE/PI/ergosterol (5 : 2.5 : 2.5 : 1, w/w/w/w) phospholipids, which mimic the outer leaflet of the plasma membrane of *C. albicans*.

To examine whether anti-*Candida* activity of K_9L_8W and D_9-K_9L_8W might depend on the peptide ability to permeate fungal membranes, we measured the influence of peptides on calcein leakage from PC/PE/PI/ergosterol (5 : 2.5 : 2.5 : 1, w/w/w/w) LUVs. K_9L_8W was able to induce almost 100% calcein leakage at a peptide : lipid molar ratio of 1 : 16, whereas D_9-K_9L_8W caused only 25% dye leakage even at a peptide : lipid molar ratio of 1 : 2 (Figure 4). A low ability to facilitate fluorescent marker escape from *C. albicans* membrane-mimicking vesicles suggested that the ultimate target site of D_9-K_9L_8W is not the cell membrane but an as yet unidentified target localized in the cytoplasm of *C. albicans*.

Therefore, to visualize the association of the peptides with *C. albicans*, we incubated *C. albicans* with FITC-labeled peptides and then visualized their cellular localization by confocal laser-scanning microscopy. FITC-labeled D_9-K_9L_8W penetrated the cell wall and cell membrane and accumulated inside the cells, whereas FITC-labeled K_9L_8W did not penetrate but associated with the membranes (Figure 5). This finding indicates that the major site of action of K_9L_8W and D_9-K_9L_8W is the membrane and the cytoplasm of *C. albicans*, respectively.

Taken together, our results demonstrated that the candidacidal activity of K_9L_8W and D_9-K_9L_8W may be due to the formation of the transmembrane pore/channel or disrupting of the fungal cytoplasmic membranes and inhibition of the intracellular functions, respectively. D_9-K_9L_8W with potent anti-*Candida* activity but no hemolytic activity may be potentially a useful lead compound for the development of novel antifungal agents.

References

1 Zasloff M. Antimicrobial peptides of multicellular organisms. *Nature* 2002; **415**: 389–395.
2 Hancock RE, Scott MG. The role of antimicrobial peptides in animal defenses. *Proc. Nat. Acad. Sci. U.S.A.* 2000; **97**: 8856–8861.
3 Hancock RE, Diamond G. The role of cationic antimicrobial peptides in innate host defences. *Trends Microbiol.* 2000; **8**: 402–410.
4 Andreu D, Rivas L. Animal antimicrobial peptides: an overview. *Biopolymers* 1998; **47**: 415–433.
5 Tossi A, Sandri L, Giangaspero A. Amphipathic, α-helical antimicrobial peptides. *Biopolymers* 2000; **55**: 4–30.
6 Helmerhorst EJ, Reijnders IM, Van't Hof W, Veerman EC, Nieuw AV. A critical comparison of the hemolytic and fungicidal activities of cationic antimicrobial peptides. *FEBS Lett.* 1999; **449**: 105–110.
7 Oren Z, Shai Y. Cyclization of a cytolytic amphipathic α-helical peptide and its diastereomer: effect on structure, interaction with model membranes, and biological function. *Biochemistry* 2000; **39**: 6103–6114.
8 Dathe M, Meyer J, Beyermann M, Maul B, Hoischen C, Bienert M. General aspects of peptide selectivity towards lipid bilayers and cell membranes studied by variation of the structural parameters of amphipathic helical model peptides. *Biochim. Biophys. Acta* 2002; **1558**: 171–186.
9 Song YM, Yang ST, Lim SS, Kim Y, Hahm KS, Kim JI, Shin SY. Effects of L- or D-Pro incorporation into hydrophobic or hydrophilic helix face of amphipathic α-helical model peptide on structure and cell selectivity. *Biochem. Biophys. Res. Commun.* 2004; **314**: 615–621.
10 Zhu WL, Song YM, Park Y, Park KH, Yang ST, Kim JI, Park IS, Hahm KS, Shin SY. Substitution of the leucine zipper sequence in melittin with peptoid residues affects self-association, cell selectivity, and mode of action. *Biochim. Biophys. Acta* 2007; **1768**: 1506–1517.
11 Matsuzaki K. Control of cell selectivity of antimicrobial peptides. *Biochim. Biophys. Acta* 2009; **1788**: 1687–1692.
12 Shai Y, Oren Z. Diastereoisomers of cytolysins, a novel class of potent antibacterial peptides. *J. Biol. Chem.* 1996; **271**: 7305–7308.
13 Oren Z, Shai Y. Selective lysis of bacteria but not mammalian cells by diastereomers of melittin: structure–function study. *Biochemistry* 1997; **36**: 1826–1835.
14 Oren Z, Hong J, Shai Y. A repertoire of novel antibacterial diastereomeric peptides with selective cytolytic activity. *J. Biol. Chem.* 1997; **272**: 14643–14649.
15 Sharon M, Oren Z, Shai Y. Anglister J. 2D-NMR and ATR-FTIR study of the structure of a cell-selective diastereomer of melittin and its orientation in phospholipids. *Biochemistry* 1999; **38**: 15305–15316.
16 Hong J, Oren Z, Shai Y. Structure and organization of hemolytic and nonhemolytic diastereomers of antimicrobial peptides in membranes. *Biochemistry* 1999; **38**: 16963–16973.
17 Papo N, Oren Z, Pag U, Sahl HG, Shai Y. The consequence of sequence alteration of an amphipathic α-helical antimicrobial peptide and its diastereomers. *J. Biol. Chem.* 2002; **277**: 33913–33921.
18 Braunstein A, Papo N, Shai Y. In vitro activity and potency of an intravenously injected antimicrobial peptide and its DL amino acid analog in mice infected with bacteria. *Antimicrob. Agents Chemother.* 2004; **48**: 3127–3129.
19 Zhu WL, Nan YH, Hahm KS, Shin SY. Cell selectivity of an antimicrobial peptide melittin diastereomer with D-amino acid in the leucine zipper sequence. *J. Biochem. Mol. Biol.* 2007; **40**: 1090–1094.
20 Wang P, Nan YH, Yang ST, Kang SW, Kim Y, Park IS, Hahm KS, Shin SY. Cell selectivity and anti-inflammatory activity of a Leu/Lys-rich α-helical model antimicrobial peptide and its diastereomeric peptides. *Peptides* 2010; **31**: 1251–1261.
21 Cannon RD, Holmes AR, Mason AB, Monk BC. Oral candida: clearance, colonization or candidiasis? *J. Dent. Res.* 1995; **74**: 1152–1161.
22 Odds FC. Candida infections: an overview. *Crit. Rev. Microbiol.* 1987; **15**: 1–5.
23 Prasad R, Kapoor K. Multidrug resistance in yeast *Candida*. *Int. Rev. Cytol.* 2005; **242**: 215–248.
24 Mochon AB, Liu H. The antimicrobial peptide histatin-5 causes a spatially restricted disruption on the *Candida albicans* surface, allowing rapid entry of the peptide into the cytoplasm. *PLoS Pathog.* 2008; **4**: 1–12.
25 Viejo-Díaz M, Andrés MT, Fierro JF. Different anti-*Candida* activities of two human lactoferrin-derived peptides, Lfpep and Kaliocin-1. *Antimicrob. Agents Chemother.* 2005; **49**: 2583–2588.
26 Benincasa M, Scocchi M, Pacor S, Tossi A, Nobili D, Basaglia G, Busetti M, Gennaro R. *J. Antimicrob. Chemother.* 2006; **58**: 950–959.
27 Shai Y. Bach D, Yanovsky A. Channel formation properties of synthetic pardaxin and analogues. *J. Biol. Chem.* 1990; **265**: 20202–20209.
28 Avrahami D, Shai Y. Conjugation of a magainin analogue with lipophilic acids controls hydrophobicity, solution assembly, and cell selectivity. *Biochemistry* 2002; **41**: 2254–2263.
29 Makovitzki A, Avrahami D, Shai Y. Ultrashort antibacterial and antifungal lipopeptides. *Proc. Nat. Acad. Sci. U.S.A.* 2006; **103**: 15997–6002.
30 Verkleij AJ, Zwaal RF, Roelofsen B, Comfurius P, Kastelijn D, Deenen LV. The asymmetric distribution of phospholipids in the human red cell membrane. A combined study using phospholipases and freeze-etch electron microscopy. *Biochim. Biophys. Acta.* 1973; **323**: 178–193.
31 Mao D, Wallace BA. Differential light scattering and absorption flattening optical effects are minimal in the circular dichroism spectra of small unilamellar vesicles. *Biochemistry* 1984; **23**: 2667–2673.
32 De Kroon AI, Soekarjo MW, De Gier J, De Kruijff B. The role of charge and hydrophobicity in peptide–lipid interaction: a comparative study based on tryptophan fluorescence measurements combined with the use of aqueous and hydrophobic quenchers. *Biochemistry* 1990; **29**: 8229–8240.
33 Zhao H, Kinnunen PK. Binding of the antimicrobial peptide temporin L to liposomes assessed by Trp fluorescence. *J. Biol. Chem.* 2002; **277**: 25170–25177.
34 Barlett CR. Phosphorus assay in column chromatography. *J. Biol. Chem.* 1959; **234**: 466–468.

